ELSEVIER

Materials Science and Engineering A 459 (2007) 137–144

MATERIALS SCIENCE & ENGINEERING A

www.elsevier.com/locate/msea

Tensile properties and fracture mechanism of Al–Mg alloy subjected to equal channel angular pressing

D.R. Fang [a,b], Q.Q. Duan [b], N.Q. Zhao [a], J.J. Li [a], S.D. Wu [b], Z.F. Zhang [b,*]

[a] *School of Materials Science and Engineering, Tianjin University, 92 Weijin Road, Tianjin 300072, People's Republic of China*
[b] *Shenyang National Laboratory for Materials Science, Institute of Metal Research, Chinese Academy of Sciences, 72 Wenhua Road, Shenyang 110016, People's Republic of China*

Received 20 October 2006; received in revised form 19 December 2006; accepted 11 January 2007

Abstract

Casting Al–2.77 wt.% Mg alloy was subjected to equal channel angular pressing (ECAP) and subsequent low-temperature annealing treatment. Tensile properties and fracture modes of as-ECAPed and annealed samples were investigated. It is found that the strength of the Al–Mg alloy increases with increasing the number of ECAP passes, while its elongation decreases. After annealing, the elongation is recovered to a large extent, consequently, the static toughness of the alloy is enhanced by a combination of ECAP and annealing treatment. Vickers hardness HV of the Al–Mg alloy monotonously increases with increasing the number of ECAP passes and follows a relationship of $HV/\sigma_b \approx 2.5$, independent of the number of ECAP passes. Meanwhile, it is noted that the casting alloy only exhibits necking before failure, while the alloy subjected to ECAP fails in shear mode, with an increasing shear fracture angle at high number of ECAP passes. Besides, the low temperature annealing treatment hardly affects the tensile fracture mode of the ECAPed alloy. Based on the experimental results above, the tensile failure mechanisms of the ECAPed Al–Mg alloy are discussed.

Keywords: Al–Mg alloy; Equal channel angular pressing (ECAP); Strength; Elongation; Static toughness; Hardness; Shear fracture

1. Introduction

At present, equal channel angular pressing (ECAP) technique has been paid much attention as a method of severe plastic deformation, and has been widely applied to various metals and alloys [1–8]. The ECAP process can apply a large shear strain to materials through a specially designed die having two equally sized channels connected at a finite angle, so a remarkable grain refinement occurs by repeated shear deformation [9–12]. The technology has been proven to be very useful for improving the mechanical properties of materials, including enhanced superplasticity, high strength and so on [2,13,14].

For Al alloys, high strength can be obtained by ECAP in the solid solution state with post-ECAP aging treatment, which is a popular technology. For example, in the case of the 2024 Al alloy [15] treated by above-mentioned process, yield strength as high as 630 MPa has been achieved. In addition, the highest yield strength (650 MPa) was obtained for 7075 Al alloy [16] using this technology. Another process is that ECAP, when performed on heated specimens, can result in enhanced strength and moderate ductility. For instance, 5052 Al alloy may have a yield strength of 394 MPa and reasonable tensile elongation when pressed at 423 K [17]. Besides, there are many other studies mainly concentrated on the property improvement and microstructure evolution of the Al alloys after ECAP. However, so far there is few report on the deformation and fracture mechanism of ECAPed Al alloy in detail, which may establish possible connection between the mechanical properties and failure modes of the investigated materials.

In the present research, one group of casting Al–Mg alloy was directly subjected to ECAP. Meanwhile, another group of Al–Mg alloy was subjected to ECAP and subsequent low temperature annealing. The main reason for low temperature annealing is to effectively recover the microstructure without losing the strain hardening ability caused by ECAP completely. On one hand, it is expected that good comprehensive mechanical properties can be achieved by a combination of multiple-pass pressing and low temperature annealing. On the other hand, the

* Corresponding author. Tel.: +86 24 23971043; fax: +86 24 23891320.
E-mail address: zhfzhang@imr.ac.cn (Z.F. Zhang).

0921-5093/$ – see front matter © 2007 Elsevier B.V. All rights reserved.
doi:10.1016/j.msea.2007.01.062

tensile deformation and fracture mechanisms of the ECAPed Al–Mg alloy are carefully investigated for better understanding of the effect of ECAP and annealing treatment.

2. Experimental procedure

Casting Al–2.77 wt.% Mg ingots were used for the current experiments. Firstly, the ingots were made into some rods of 10 mm in diameter and 80 mm in length by spark cutting technique. Secondly, equal channel angular pressing (ECAP) was conducted at room temperature using a solid die having an angle of 90° between the two channels. The samples subjected to repetitive pressing were rotated by 90° in the same direction between each pass in the procedure designated as route B_C [18]. Before pressing, the rods were coated with MoS_2 as lubricant. The number of ECAP passes is one, two and four, respectively. Some of the as-ECAP-processed samples were annealed at 523 K for 90 min. Subsequently, a small piece was cut from each sample for hardness test. The Vickers hardness was measured with a MVK-H3 Vickers hardness tester using a load of 50 g holding for 10 s.

Tensile specimens with gauge length and cross-section of 14 mm and 3 mm × 5 mm were machined from the ECAPed samples with their tensile axes lying parallel to the pressing direction. The vertical plane parallel to extrusion direction is defined as *Y*-plane. Tensile specimens were mechanically polished followed by electropolishing in a solution of $HClO_4$ and C_2H_5OH. These specimens were subjected to tensile load up to failure at room temperature using MTS mini testing machine operating at a constant rate of cross-head displacement with a strain rate of about $5 \times 10^{-4}\ s^{-1}$.

The microstructure observations were performed using a S360 Cambridge scanning electron microscopy (SEM) and a JEM-2000FX II transmission electron microscopy (TEM). The thin foils for TEM observations were cut from the center of the pressed rods on the *Y*-plane, then were mechanically ground to about 50 μm thick and finally thinned by twin-jet electropolishing method with a solution of 33% nitric acid–methanol. After tensile fracture, all the samples were observed by SEM to reveal the deformation and fracture features.

3. Results and discussion

3.1. Microstructures before and after ECAP

Fig. 1(a) shows the microstructure of the casting Al–2.77 wt.% Mg alloy. There is only one phase, i.e. Al solid solution, and the average grain size is about 100–200 μm. After ECAP, the grains have been refined to submicron-meter level after four passes, as shown in Fig. 1(b), and high dislocation density within the grains can be observed. After annealing at 523 K for 90 min, the dislocation density obviously decreases and a duplex microstructure with recrystallized and unrecrystallized areas appears, showing a bimodal distribution of grain size [19]. Wang et al. [20] and Morris and Munoz-Morris [21] have investigated the microstructure of ECAPed Al–3% Mg and its evolution during annealing in detail, the present research is consistent with their results. However, it is noted that the similar microstructure could be acquired by the simpler process without rolling [20] and homogenization [21] before ECAP.

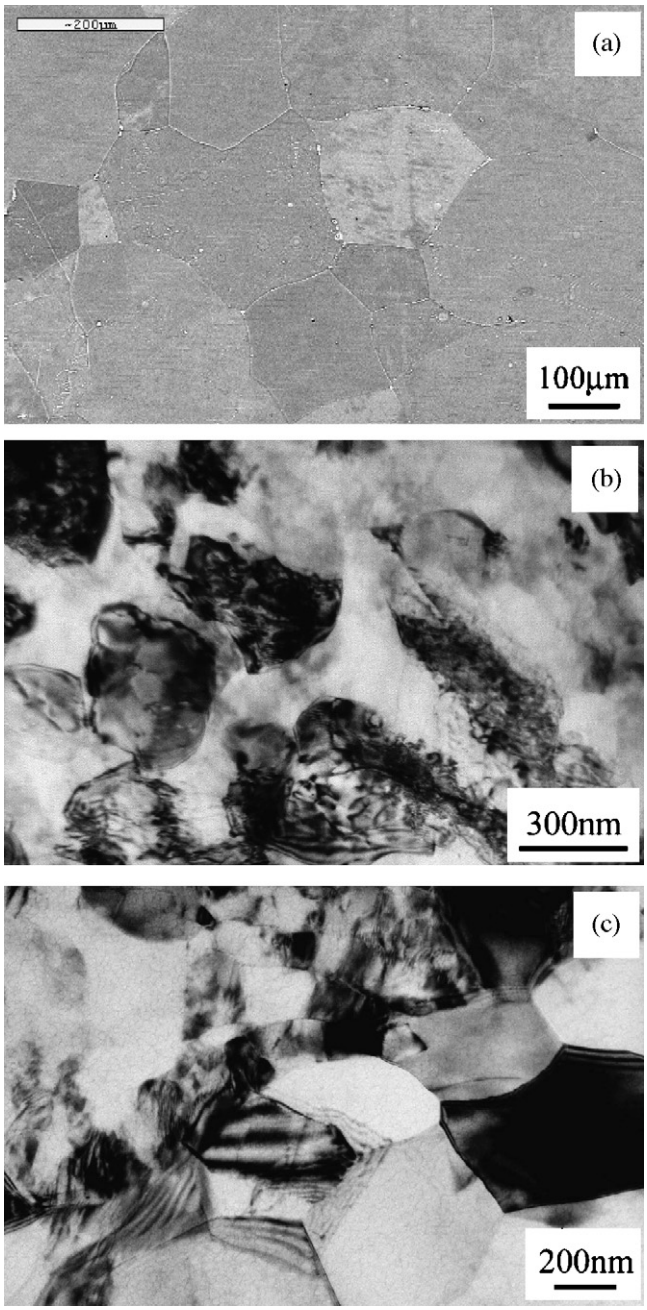

Fig. 1. Microstructures of Al–2.77% Mg alloy. (a) As-cast, (b) ECAPed for four pass (observed on *Y*-plane) and (c) ECAPed for four pass and subsequent annealing at 523 K for 90 min (observed on *Y*-plane).

3.2. Tensile properties

Fig. 2 shows the tensile stress–strain curves of the Al–Mg samples. It can be seen from Fig. 2(a) that, the strength of the alloy increases clearly with increasing the number of ECAP passes due to grain refinement and the continuous increase in

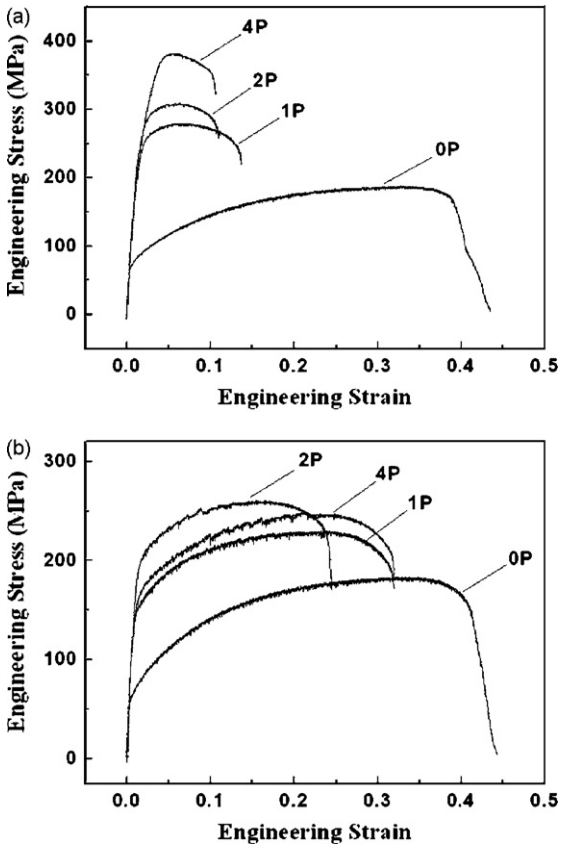

Fig. 2. Tensile stress–strain curves of Al–2.77% Mg alloy subjected to (a) ECAP and (b) ECAP + annealing.

dislocation density. For the as-cast Al–Mg alloy, the ultimate tensile strength (UTS) is about 190 MPa after one pass and reaches about 380 MPa after four passes. However, its elongation decreases from 43% (as-cast) to 10% (four passes). For the samples after annealing, the UTS and elongation show the similar variation trend to those of samples only subjected to ECAP (see Fig. 2(b)). It should be noted that the strength hardly changes while the elongation increases after four passes and subsequent annealing, as clearly seen in Fig. 2(a) and (b). From Fig. 3(a) and (b), it is noted that the strength of the Al–Mg alloy decreases while the elongation is obviously improved after annealing at 523 K. For example, the sample pressed for four passes and annealed, the strength is about 250 MPa and the elongation can be improved to about 32%. It is obvious that when the Al–Mg alloy was treated by ECAP and subsequent low-temperature annealing, its elongation has been recovered to a large extent, while a high strength is still retained. This high elongation can be explained by the bimodal distribution of grain size in the ECAPed and subsequently annealed samples [19]. Compared with the other Al alloy [15,16] ECAPed in the solid solution state with post-aging treatment and 5052 Al alloy [17] ECAPed in heating state, the strength of the current Al–Mg alloy is lower, but the elongation is much better.

Fig. 3(c) shows the variation of static toughness of the Al–Mg alloy with the number of ECAP passes. Static toughness represents comprehensive mechanical property of materials, and indicates a combination of materials' strength and plasticity.

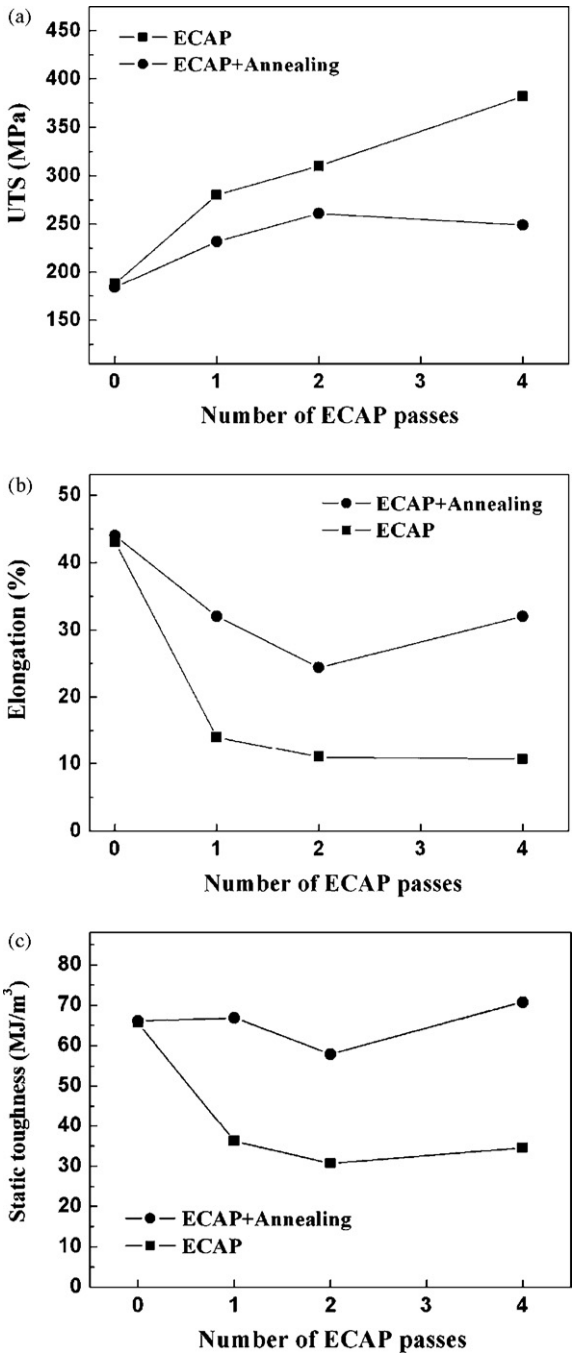

Fig. 3. Dependence of (a) ultimate tensile strength, (b) elongation and (c) static toughness on the number of ECAP passes for Al–2.77% Mg alloy.

The static toughness U of materials can be calculated by

$$U = \int_0^{\varepsilon_f} \sigma \, d\varepsilon, \tag{1}$$

where σ is the flow stress and ε_f is the total strain at fracture. The static toughness was rarely mentioned in the study on the mechanical properties of the ECAPed materials. It can be seen that the static toughness of the casting Al–Mg alloy is about 65 MJ/m^3, after one ECAP pass its static toughness decreases significantly. It can be explained that its elongation is lower than that in casting state, although its strength is obviously improved.

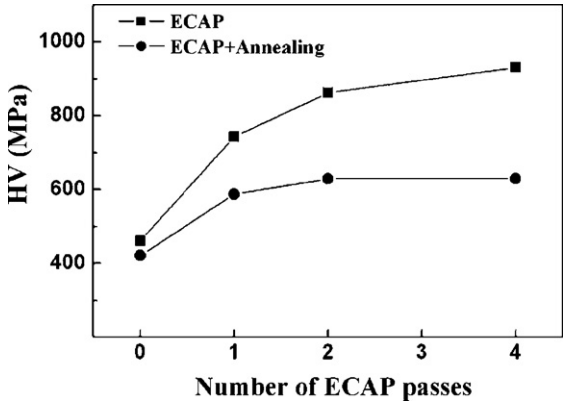

Fig. 4. Dependence of Vickers hardness on the number of ECAP passes for Al–2.77% Mg alloy.

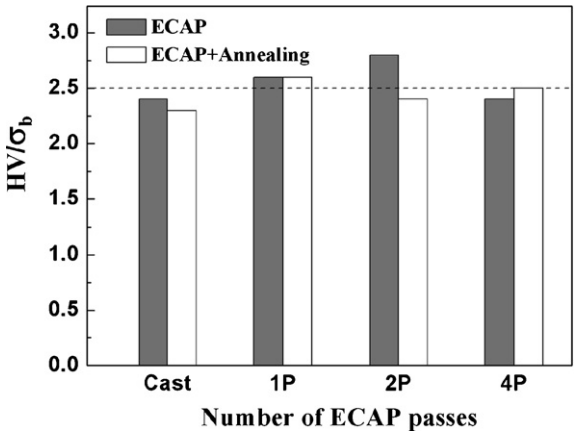

Fig. 5. Dependence of the ratio HV/σ_b on the number of ECAP passes for Al–2.77% Mg alloy.

Furthermore, it is evident that the static toughness of the samples subjected to ECAPed and annealed is always higher than that of the samples without post-annealing. When the Al–2.77% Mg alloy was pressed for four passes and annealed, its static toughness reaches 70 MJ/m^3, slightly higher than that of the as-cast alloy. In addition, for Al–Cu alloy [22] subjected to ECAP, its static toughness was also enhanced after multiple passes. Besides, the static toughness of the Al–2.77% Mg alloy is higher than that of 7075 Al alloy [16] ECAPed in the solid solution state with post-ECAP aging treatment and 5052 Al alloy [17] ECAPed in heating state. So it is suggested that it is feasible to adjust the comprehensive mechanical properties of materials by a combination of ECAP and post-annealing treatment.

3.3. Relationship between hardness and strength

Fig. 4 shows Vickers hardness HV as a function of the number of ECAP passes. It is evident that the hardness increases with increasing the number of ECAP passes due to grain refinement and work hardening. While annealing treatment causes a decrease in hardness of the samples subjected to different number of ECAP passes. This variation trend of hardness is similar to that of strength. Previous investigations have shown that the hardness of materials is proportional to the yield strength with a relationship of $HV \approx 3\sigma_y$. Based on the relationship, Furukawa et al. [23] once studied the Hall–Petch relationship in an Al–3% Mg alloy subjected to ECAP, by measuring the hardness of as-fabricated and statically annealed specimens. It is shown that the data exhibit an apparent decrease in hardness with increasing annealing temperature after ECAP, and the Hall–Petch relationship persists down to at least the finest grain size (90 nm).

In order to investigate the relationship between Vickers hardness and fracture strength σ_b of ECAPed Al–2.77% Mg alloy, the ratio HV/σ_b of the Al–Mg samples subjected to different number of ECAP passes was calculated and is shown in Fig. 5. It can be seen that the ratio HV/σ_b is close to 2.5 for the casting and ECAPed Al–2.77% Mg alloys, independent of the number of passes, and so is the ratio for the samples after annealing. This indicates that the ratio HV/σ_b of Vickers hardness to UTS of the ECAPed Al–Mg alloy also maintains a constant value of 2.5, which is a little bit smaller than the ratio $HV/\sigma_y = 3$ of Vickers hardness to yield strength for the bulk metallic glassy materials as discussed by Pan et al. [24].

3.4. Deformation and fracture morphologies

Fig. 6 shows the macro-scale fracture morphology of the Al–Mg alloy subjected to different number of ECAP passes. The casting specimen exhibits obvious necking before failure, as clearly seen in Fig. 6(a). While after ECAP, the fracture becomes shear mode due to strong work-hardening effect. After one pass, the shear fracture plane makes an angle of about 50° with respect to the tensile direction (Fig. 6(b)). After two and four passes, the shear fracture angles are 53° and 58° (Fig. 6(c) and (d)), respectively. The change from necking fracture in casting state to shear fracture after ECAP provides strong evidence that the plasticity of the Al–Mg alloy decreases as a result of work hardening. It can be seen from Fig. 7 that the fracture displays the similar character for the samples after ECAP and subsequent annealing. The shear fracture angles are almost equal for the samples before and after every pass. So low temperature annealing treatment does not obviously affect the tensile fracture mode of the ECAPed Al–2.77% Mg alloy.

Fig. 8 is the fracture surface morphology of the Al–Mg alloy subjected to different number of ECAP passes. All specimens failed in a ductile manner, consisting of numerous dimples over the entire surface. Dimples are slightly elongated along shear direction after ECAP, as observed in Fig. 8(b)–(d). The elongated dimples should be a result of the void nucleation and subsequent coalescence by strong shear deformation and fracture process on the shear plane. In addition, it can be seen that the average dimple size of the cast specimen is tens of microns, whereas the average dimple size gradually decreases with increasing the number of ECAP passes, and becomes about several microns after four passes. For the Al–Mg alloys subjected to ECAP and subsequent annealing, the fracture character and dimple size are similar, as seen in Fig. 9 in detail. According to the previous research [25,26], the continuous decrease in the dimple size can be explained by grain refinement as well as work-hardening and the fragmentation of the second particles caused by ECAP.

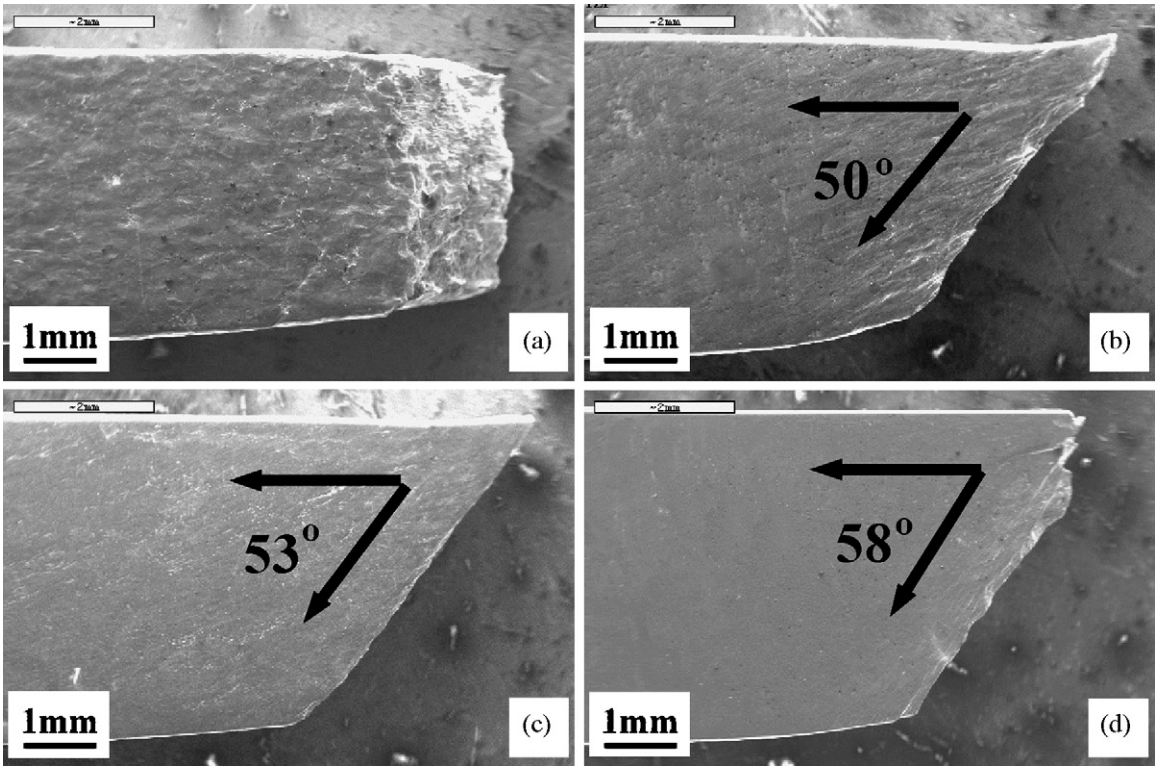

Fig. 6. Fracture morphology of Al–2.77% Mg alloy observed on *Y*-plane. (a) As-cast and ECAPed for (b) one pass, (c) two passes and (d) four passes.

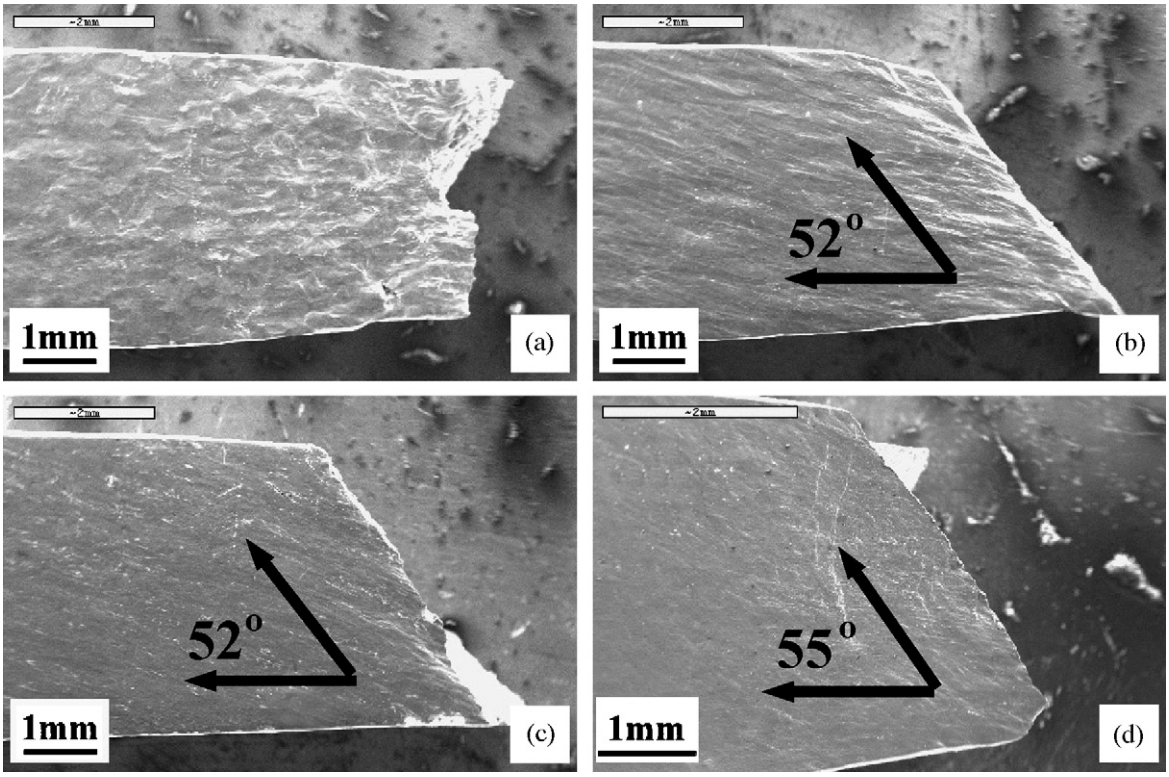

Fig. 7. Fracture morphology of Al–2.77% Mg alloy after annealing observed on *Y*-plane. (a) As-cast and ECAPed for (b) one pass, (c) two passes and (d) four passes.

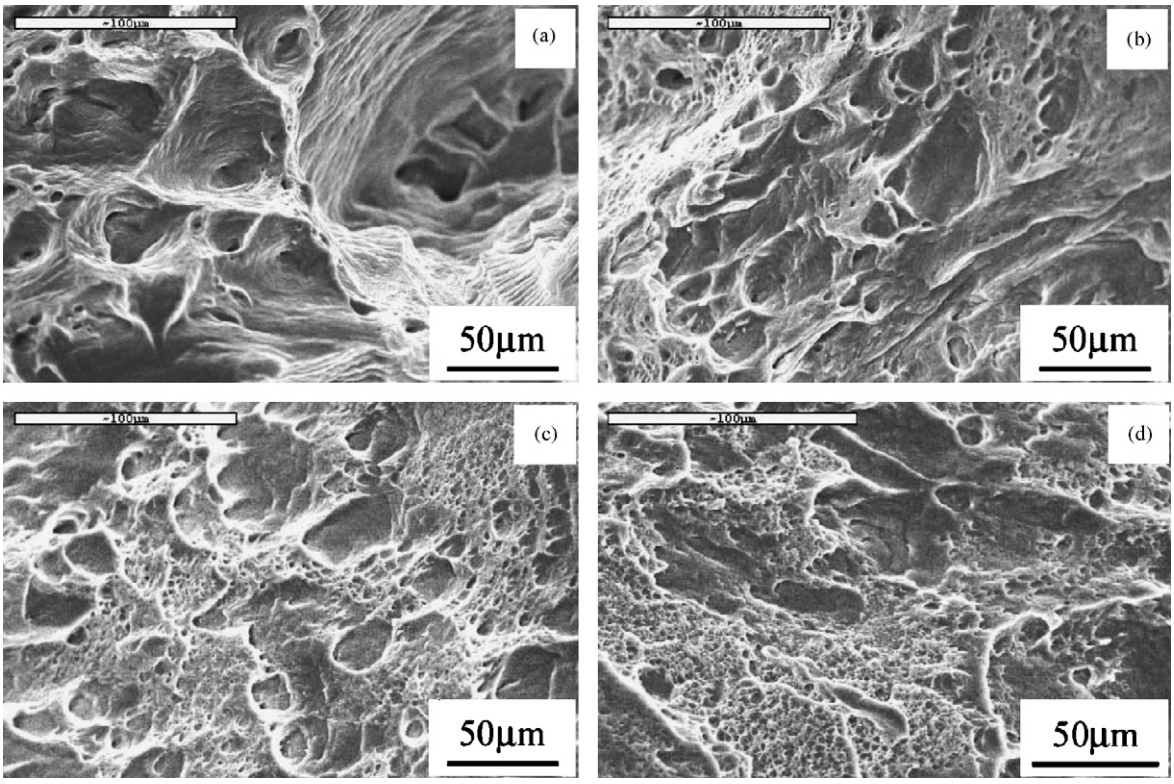

Fig. 8. Fracture surface morphology of Al–2.77% Mg alloy. (a) As-cast and ECAPed for (b) one pass, (c) two passes and (d) four passes.

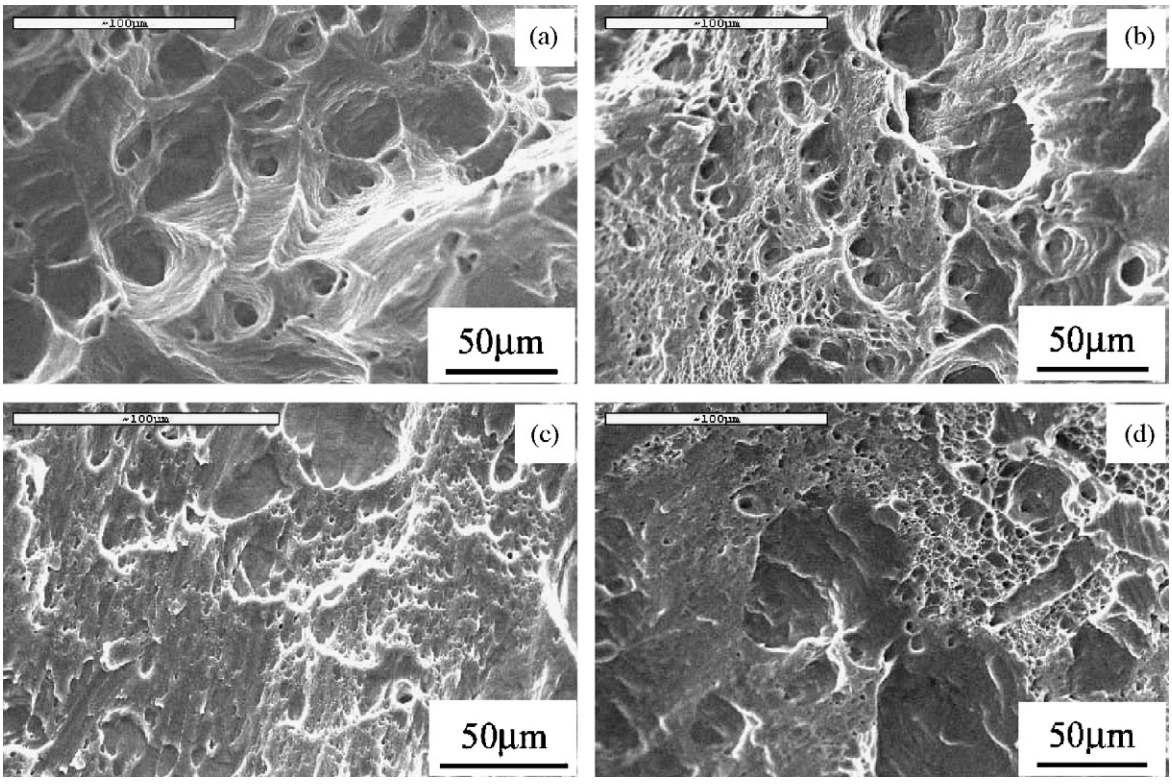

Fig. 9. Fracture surface morphology of Al–2.77% Mg alloy after annealing. (a) As-cast and ECAPed for (b) one pass, (c) two passes and (d) four passes.

3.5. Fracture mechanism

From the observations in Figs. 6 and 7, it is apparent that the specimens subjected to ECAP treatment always fail in a shear fracture mode. Meanwhile, an interesting phenomenon is that all the shear fracture angles are obviously larger than 45°, indicating that the shear fracture does not occur along the maximum shear stress plane. In return, the fracture of the ECAPed Al–Mg alloys neither follows the maximum normal stress criterion nor obeys the Tresca criterion. Therefore it is suggested that both normal and shear stresses (σ_n and τ_n) on the shear plane control the failure of the ECAPed specimens, and they can be expressed as [27]:

$$\sigma_n = \sigma_T \sin^2 \theta_T, \tag{2a}$$

$$\tau_n = \tau_T \sin \theta_T \cos \theta_T, \tag{2b}$$

where σ_T is the tensile stress and θ_T is the shear fracture angle of the specimen. For better understanding the shear fracture mechanism, as illustrated in Fig. 10, a unified tensile fracture criterion [28] was proposed as below:

$$\left(\frac{\sigma_n}{\sigma_0}\right)^2 + \left(\frac{\tau_n}{\tau_0}\right)^2 = 1, \tag{3}$$

where σ_0 and τ_0 are the average critical normal fracture stress and the shear fracture stress of the material. According to the unified tensile fracture criterion, τ_0 and σ_0 can be calculated by the following equations:

$$\sigma_T = 2\tau_0\sqrt{1-\alpha^2}, \tag{4}$$

$$\theta_T = \frac{\pi}{2} - \frac{1}{2}\arctan\left(\frac{\sqrt{1-2\alpha^2}}{\alpha^2}\right), \tag{5}$$

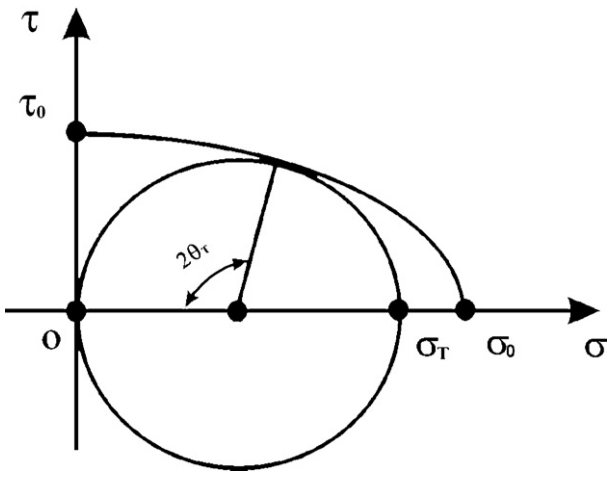

Fig. 10. Illustration of shear fracture angles variation according to unified tensile fracture criterion.

$$\alpha = \frac{\tau_0}{\sigma_0}, \tag{6}$$

where the ratio $\alpha = \tau_0/\sigma_0$ is a fracture mode factor controlling the macro-scale fracture modes of the materials. It is suggested that when $0 < \alpha = \tau_0/\sigma_0 < \sqrt{2}/2$, shear fracture angle θ_T is in the range of 45–90° [28]. The ratios α of the samples subjected to different number of ECAP passes were calculated and are listed in Table 1. From the data in Table 1, the value α should be in the scope of $0 < \alpha < \sqrt{2}/2$. Consequently, depending on the ratio α, the shear fracture angles range about from 50° to 60°, as shown in Figs. 6 and 7.

According to the unified tensile fracture criterion, the variation of the average critical normal and shear stresses (σ_0 and τ_0) on the number of ECAP passes were calculated and are shown in Fig. 11. It is apparent that τ_0 hardly changes, while σ_0 obviously decreases from one pass to two passes (see Fig. 11(a)).

Table 1
Ratio α for samples subjected to different number of ECAP passes

	One pass	Two passes	Four passes	One pass + annealing	Two passes + annealing	Four passes + annealing
Shear fracture angle, θ_T (°)	50	53	58	52	52	55
$\alpha = \tau_0/\sigma_0$	0.384	0.464	0.552	0.441	0.441	0.504

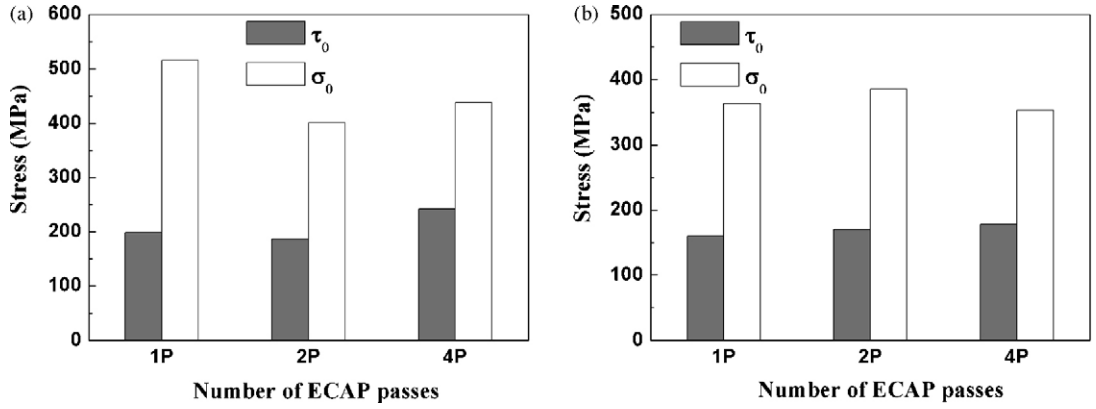

Fig. 11. Dependence of τ_0 and σ_0 on the number of ECAP passes for Al–2.77% Mg alloy. (a) As-ECAP and (b) ECAP + annealing.

While from two passes to four passes, τ_0 and σ_0 increase simultaneously, from 185 MPa to 242 MPa (τ_0) and from 400 MPa to 438 MPa (σ_0). It is evident that the increasing proportion of τ_0 is higher than that of σ_0, resulting in an increased ratio $\alpha = \tau_0/\sigma_0$. Since the shear fracture angle θ_T is a function of the ratio $\alpha = \tau_0/\sigma_0$ (see Eq. (5)), it is not difficult to understand why the shear fracture angle increases with increasing the number of ECAP passes, as shown in Fig. 6(a)–(d).

After annealing, both τ_0 and σ_0 decrease for the samples subjected to different number of ECAP passes, as shown in Fig. 11(b). It can be seen that τ_0 increases from 160 MPa to 170 MPa, and σ_0 also increases from 363 MPa to 385 MPa from one pass to two passes. Moreover, it is noted that the increasing proportion is equal (about 6%) for both τ_0 and σ_0, so the ratio α nearly maintains constant. Accordingly, the shear fracture angles are both 52° after one pass and two passes. Thereafter, τ_0 increases while σ_0 decreases after four passes, leading to the increase in the ratio α again. As a result, the shear fracture angles change less, from 52° after one pass to 55° after four passes.

Based on the failure modes above, it is suggested that the ECAP process can effectively change the fracture mode from necking to shear fracture with different shear fracture angles, which indicates a different variation tendency for average critical normal and shear fracture stresses. Furthermore, the ECAP process can modulate the mechanical properties of the materials with different strength, elongation, static toughness and failure mode.

4. Conclusions

(1) The UTS of Al–2.77% Mg alloy increases with increasing the number of ECAP passes, while the elongation decreases. After annealing, the elongation is recovered to a large extent. Consequently, the static toughness of the alloy is enhanced by a combination of ECAP and annealing treatment.
(2) The Vickers hardness HV of the Al–2.77% Mg alloy approximately obeys the relationship $HV/\sigma_b \approx 2.5$, independent of the number of ECAP passes, and so is that for the samples after annealing.
(3) The casting specimen exhibits obvious necking before failure, while after ECAP, the specimens fail in a shear mode. And all shear fracture angles are larger than 45° and increase with increasing the number of ECAP passes. This indicates that the shear fracture of the ECAPed Al–Mg alloy is controlled by both shear and normal stresses.

Acknowledgements

The authors would like to thank W. Gao, H.H. Su, J.L. Wen, F.F. Wu, G. Yao, and P. Zhang for the assistance in the mechanical tests, SEM observations and stimulating discussions on the manuscript. This work was supported by "Hundred of Talents Project" of the Chinese Academy of Sciences, and the National Natural Science Foundation of China (NSFC) under grant no. 50571102 and the National Outstanding Young Scientist Foundation for Z.F. Zhang under Grant no. 50625103.

References

[1] V.M. Segal, Mater. Sci. Eng. A197 (1995) 157.
[2] Z. Horita, M. Furukawa, M. Nemoto, A.J. Barnes, T.G. Langdon, Acta Mater. 48 (2000) 3633.
[3] A. Vinogradov, V. Patlan, Y. Suzuki, K. Kitagawa, V.I. Kopylov, Acta Mater. 50 (2002) 1639.
[4] W.J. Kim, C.W. An, Y.S. Kim, S.I. Hong, Scripta Mater. 47 (2002) 39.
[5] Z.F. Zhang, S.D. Wu, Y.J. Li, S.M. Liu, Z.G. Wang, Mater. Sci. Eng. A412 (2005) 279.
[6] G.I. Raab, E.P. Soshnikova, R.Z. Valiev, Mater. Sci. Eng. A387–389 (2004) 674.
[7] J.T. Wang, C. Xu, Z.Z. Du, G.Z. Qu, T.G. Langdon, Mater. Sci. Eng. A410–411 (2005) 312.
[8] C.X. Huang, K. Wang, S.D. Wu, Z.F. Zhang, G.Y. Li, S.X. Li, Acta Mater. 54 (2006) 655.
[9] V.M. Segal, Mater. Sci. Eng. A271 (1999) 322.
[10] M. Furukawa, Y. Iwahashi, Z. Horita, M. Nemoto, T.G. Langdon, Mater. Sci. Eng. A257 (1998) 328.
[11] Z.C. Wang, P.B. Prangnell, Mater. Sci. Eng. A328 (2002) 87.
[12] W.J. Kim, S.I. Hong, Y.S. Kim, S.H. Min, H.T. Jeong, J.D. Lee, Acta Mater. 51 (2003) 3293.
[13] Z. Horita, T. Fujinami, M. Nemoto, T.G. Langdon, J. Mater. Process. Technol. 117 (2001) 288.
[14] R.Z. Valiev, I.V. Alexandrov, Y.T. Zhu, T.C. Lowe, J. Mater. Res. 17 (2002) 5.
[15] W.J. Kim, C.S. Chung, D.S. Ma, S.I. Hong, H. Kim, Scripta Mater. 49 (2003) 333.
[16] Y.H. Zhao, X.Z. Liao, Y.T. Zhu, R.Z. Valiev, J. Mater. Res. 20 (2005) 288.
[17] T.L. Tsai, P.L. Sun, P.W. Kao, C.P. Chang, Mater. Sci. Eng. A342 (2003) 144.
[18] Y. Iwahashi, Z. Horita, M. Nemoto, T.G. Longdon, Acta Mater. 46 (1998) 3317.
[19] Y.M. Wang, M.W. Chen, F.H. Zhou, E. Ma, Nature 419 (2002) 912.
[20] J. Wang, Y. Iwahashi, Z. Horita, M. Furukawa, M. Nemoto, R.Z. Valiev, T.G. Langdon, Acta Mater. 44 (1996) 2973.
[21] D.G. Morris, M.A. Munoz-Morris, Acta Mater. 50 (2002) 4047.
[22] D.R. Fang, Z.F. Zhang, S.D. Wu, C.X. Huang, H. Zhang, N.Q. Zhao, J.J. Li, Mater. Sci. Eng. A426 (2006) 305.
[23] M. Furukawa, Z. Horita, M. Nemoto, R.Z. Valiev, T.G. Langdon, Acta Mater. 44 (1996) 4619.
[24] X.F. Pan, H. Zhang, Z.F. Zhang, M. Stoica, G. He, J. Eckert, J. Mater. Res. 20 (2005) 2632.
[25] A. Vinogradov, T. Ishida, K. Kitagawa, V.I. Kopylov, Acta Mater. 53 (2005) 2181.
[26] Y.G. Ko, D.H. Shin, K.T. Park, C.S. Lee, Scripta Mater. 54 (2006) 1785.
[27] Z.F. Zhang, J. Eckert, L. Schultz, Acta Mater. 51 (2003) 1167.
[28] Z.F. Zhang, J. Eckert, Phys. Rev. Lett. 94 (2005) 094301.